Estimation of accuracy achieved by ^{199}Hg co-magnetometer

Y. Arimoto, KEK

June 30, 2011

Abstract

It is aimed to measure a magnetic field in a UCN-storage bottle with the uncertainty less than 0.1 fT by using a co-magnetometer. We adopts for ^{199}Hg magnetometer as the co-magnetometer. This is one of optical pumping magnetometer and there are two types of the ^{199}Hg magnetometer, Faraday rotation method and absorption method. Accuracies of ^{199}Hg magnetometer was estimated for the Faraday rotation method and the absorption method. By the Faraday rotation method, it is estimated that shot noise limit of 0.1 fT is achieved in 8 days measurement. Light shift which causes frictional magnetic field was calculated. Requirements for a probe light to reduce the systematic error less than 0.1 fT were estimated; the allowable relative frequency fluctuation is less than 40 kHz, allowable uncertainty of absolute frequency <1.3 MHz, allowable intensity fluctuation < 3%. On the other hand, by the absorption method, it was found that it took more than 2000 days to achieve the uncertainty less than 0.1 fT.

1 Faraday rotation method

1.1 Measurement scheme

A schematic view of magnetic measurement based on the Faraday rotation method is shown in Fig. 1. Linearly polarized light travels through a ^{199}Hg vapor cell where polarized ^{199}Hg atoms are precessing at Larmor frequency. Polarized plane of transmitted light is oscillated with the frequency. The frequency determines magnetic field in the cell. In the Hg atomic

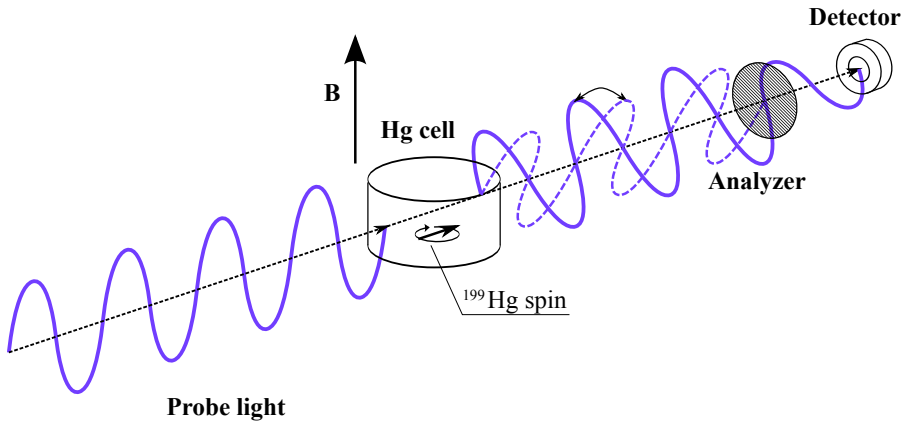

Figure 1: Schematic figure of magnetic measurement system based on the Faraday rotation method.

EDM measurement [1], a Larmor frequency of ^{199}Hg atom is measured by the same method, so this can be referred. The calculation will be done under the following conditions; a profile of the probe light and cross section of the cell is same with homo genius distribution (Fig. 2).

1.2 Measurement uncertainties of magnetic field

Main components of the measurement uncertainties of the magnetic field are shot-noise and light shift; the former one is statistical error and the latter one is systematic error.

The shot noise limit can be reduced by increasing intensity of the probe light, however the high intense light makes relax the polarization of the mercury atoms; it is limitation of intensity of the probe light.

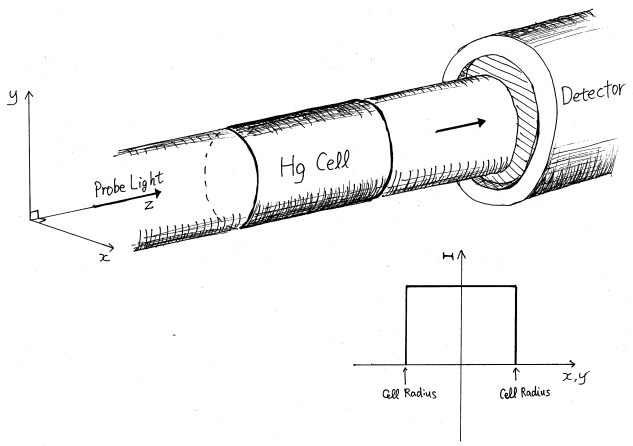

Figure 2: The profile of probe light compared with the cell.

On the other hand, light shift makes fictitious magnetic field. The magnitude of fictitious field is determined by several parameters of the probe light; intensity, frequency, incident angle with respect to quantize axis and linear polarization.

1.3 Statistical error

1.3.1 Shot noise limit

In the nEDM experiment, it is necessary that average magnetic field is measured during a Ramsey measurement. In the Ramsey measurement, precession frequency of the neutrons is measured by the Ramsey technique. The method is described in K. Green, *et al.* [2]. Here, one Ramsey measurement means the measurement of the neutron precession frequency per one filling of UCN into a storage bottle. It is expected that during the Ramsey measurement period, a magnetic field which produces a quantize axis fluctuates [2]. The average magnetic field is determined by phase difference between initial oscillation and final one in the Ramsey measurement. To simplify calculation, it is assumed that the polarization is constant and becomes to be zero after T_0. In this case, the shot noise is expressed by, (refer to appendix B)

$$\delta B = 2\pi\sigma_f/\gamma \tag{1}$$

$$= \frac{2}{A\gamma}\sqrt{\frac{\omega_L}{\pi n_{\rm cycl}\dot{N}_{\rm ph}}}\frac{1}{T_0}. \tag{2}$$

Here A is oscillation amplitude of transmitted-probe light; where it is assumed that the intensity of the probe light transmitted through the analyzer is unity, and $\dot{N}_{\rm ph}$ is number of detected photons per unit time.

1.3.2 Derivation of oscillation amplitude, A

The oscillation amplitude A in Eq. 2 is calculated with maximum angle of Faraday rotation, $\phi_{\rm rot}$ and an angle between the analyzer axis and a polarization axis of the probe light at an entrance of the cell, β as follows.

The Faraday rotation angle is written by,

$$\phi = \frac{\omega L}{2c}\left(n_+ - n_-\right), \tag{3}$$

where n_+, n_- are given by,

$$n_\pm = 1 + \frac{2\pi\alpha_{\rm f} c\mu_{\rm e}^2}{e^2}\left(g^{(3/2)}N_{\pm 1/2} + \frac{2}{3}g^{(1/2)}N_{\mp 1/2} + \frac{1}{3}g^{(3/2)}N_{\mp 1/2}\right). \tag{4}$$

Please refer to Appendix D in detail.

According to Eq.(4), calculated refraction index are shown in Fig. 3-(a),-(b). Here, the mercury density N, the length of the mercury-storage bottle is 3×10^{10} atoms/cm^{-3} and 30 cm, respectively. It is set that these values are same as the

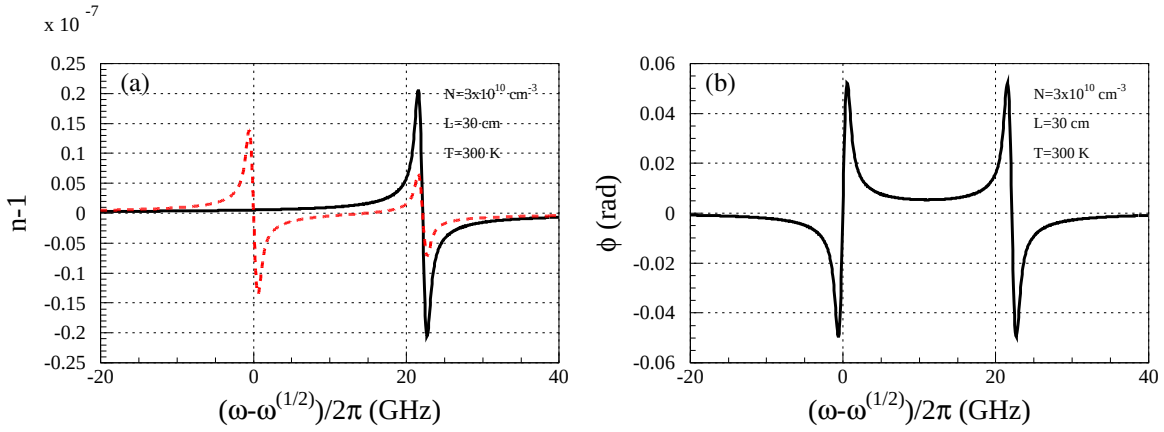

Figure 3: (a) The refractive index of ^{199}Hg atom as a function of detune of the probe light. (The solid line and dot line are $n_+ - 1$, $n_- - 1$, respectively.) (b)Faraday rotation angle as a function of detune of the probe light.

nEDM experiment at ILL [3]. The Doppler broadening is included at 300 K. Included transitions are 6^1S_0-$6^3P_1(F{=}1/2)$ and 6^1S_0-$6^3P_1(F{=}3/2)$.

From Fig 3-(b), it can be seen that the rotation angle at midway between $F = 1/2$ and $F = 3/2$ is

$$\phi_{\rm rot} = \pm 0.0053 \text{ rad.} \tag{5}$$

This value is two order smaller than the Hg-EDM experiment [4] where they search ^{199}Hg atomic EDM with Faraday rotation method; nevertheless, such a small rotation angle are usually measured in atomic magnetometers [5].

Then, the intensity of the probe light transmitted through the analyzer is expressed by [4],

$$I(t) = \frac{I_0}{2}\left[1 - \cos(2\beta) + 2\phi_{\rm rot}\sin(\omega_L t)\sin(2\beta)e^{-t/\tau}\right]. \tag{6}$$

Where β is an angle between initial polarization plane of the probe light and an axis of the analyzer. When $\beta = \pi/4$, the amplitude is maximum and

$$I(t) = \frac{I_0}{2}\left[1 + 2\phi_{\rm rot}\sin(\omega_L t)e^{-t/\tau}\right]. \tag{7}$$

As the result, the amplitude A is

$$\begin{aligned} A &= \left\{\frac{I_0}{2}\left[1 + 2\phi_{\rm rot}e^{-t/\tau}\right] - \frac{I_0}{2}\right\}/(I_0/2) && (8)\\ &= 2\phi_{\rm rot}e^{-t/\tau} && (9)\\ &= 2 \times 0.0053 && (10)\\ &= 0.0106. && (11) \end{aligned}$$

Figure 4 shows schematic signal of transmitted probe light measured by a photo detector.

1.3.3 Estimation of relaxation time T_0 for ^{199}Hg exposed to probe light

The polarization of ^{199}Hg atoms which is Larmor-precessing is relaxed due to absorption of circular-polarization component of the probe light. This limits the shot noise limit even if probe light intensity is increased. Here, the shot-noise limit will be numerically estimated.

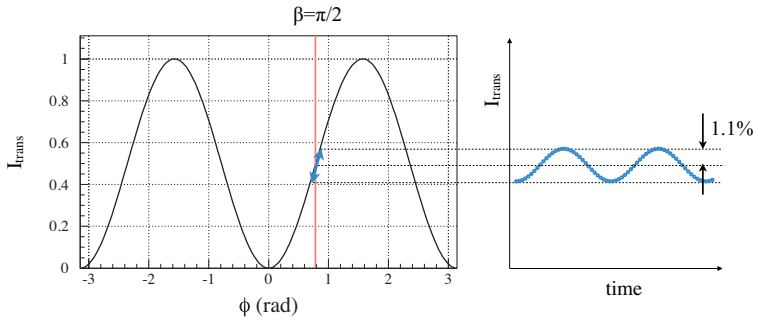

Figure 4: Faraday rotation signal. Left: Transmittance of linear polarized light which penetrate the analyzer as a function of angle between the direction of polarization plane and the analyzer angle. Right: Detected signal at the photo detector as a function of time.

The time evolution of number of density of the atomic states, 1, 2, 3, 4 (see Fig. 7) are expressed by,

$$\frac{dN_0}{dt} = (N_3 - N_0)W^-(t) - A_{\rm eg}N_0 \tag{12}$$

$$\frac{dN_1}{dt} = (N_2 - N_1)W^+(t) - A_{\rm eg}N_1 \tag{13}$$

$$\frac{dN_2}{dt} = -(N_2 - N_1)W^+(t) + \frac{2}{3}A_{\rm eg}N_1 + \frac{1}{3}A_{\rm eg}N_0 - \frac{\Gamma}{2}(N_3 - N_2) \tag{14}$$

$$\frac{dN_3}{dt} = -(N_3 - N_0)W^-(t) + \frac{2}{3}A_{\rm eg}N_0 + \frac{1}{3}A_{\rm eg}N_1 + \frac{\Gamma}{2}(N_3 - N_2) \tag{15}$$

$$W^+(t) = W_0 \cos^2 \omega t \tag{16}$$

$$W^-(t) = W_0 \sin^2 \omega t. \tag{17}$$

For simplicity, a radiation trapping process [6] is not considered in above equations. Here the quantize axis is coincide with the rotating coordinate with the Larmor frequency of ^{199}Hg atom. Then Γ is relaxation rate of the polarization of ^{199}Hg atoms and relaxation time is given by,

$$T_1 = 1/\Gamma. \tag{18}$$

Then W_0 in Eq.(16), (17) is transition rate due to photo absorption and is expressed by [7]

$$W_0 = \frac{c^2 A_{\rm eg} I_\nu}{8\pi n^2 h\nu^3} g(\nu) \tag{19}$$

$$= \frac{\alpha_\nu}{n_e - n_g}\frac{I_\nu}{h\nu} \tag{20}$$

$$= \sigma_{\rm phot}\ [\mathrm{cm}^2] \cdot \frac{I_\nu}{h\nu}\ [\mathrm{s}^{-1}\cdot\mathrm{cm}^{-2}]. \tag{21}$$

Here, α_ν, $\sigma_{\rm phot}$ are photon absorption coefficient and photon absorption cross section of ^{199}Hg, respectively and are $\sigma_{\rm phot} = 2 \times 10^{-18}$ cm^2, respectively (Appendix C).

By substituting Eq. (21) into the rate equations, relaxation rates as a function of photon flux density of the probe light are obtained and are shown in Fig. 8-(a). Shot-noise limits as a function of photon flux density of the probe light are plotted in Figs. 8-(b), -(c).

The obtained shot noise limits in Fig. 8-(c) are summarized in a Table 1.

1.3.4 Measurement time to achieve statistical error of less than 0.1 fT

Since the shot noise is statistical error, n times measurement reduces the error by $1/\sqrt{n}$. Assuming that UCN storage time is 20 sec and a Ramsey measurement is 160 sec, the measurement time is totally 180 sec. Since the Ramsey measurement will be performed by flipping magnetic field and electric field, one set measurement is $180 \times 4 = 720$ sec (Fig. 9). Since

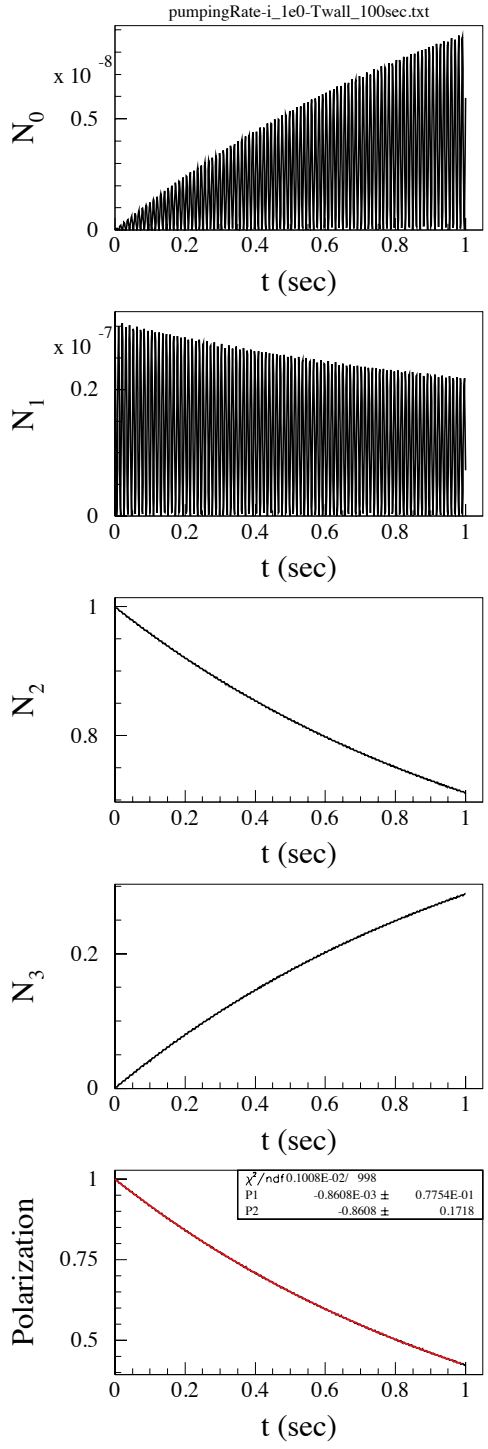

Figure 5: Time evolution of number of density of ^{199}Hg atomic states calculated by the rate equation. The probe light intensity is $I = 1$ W/cm^{-2}.

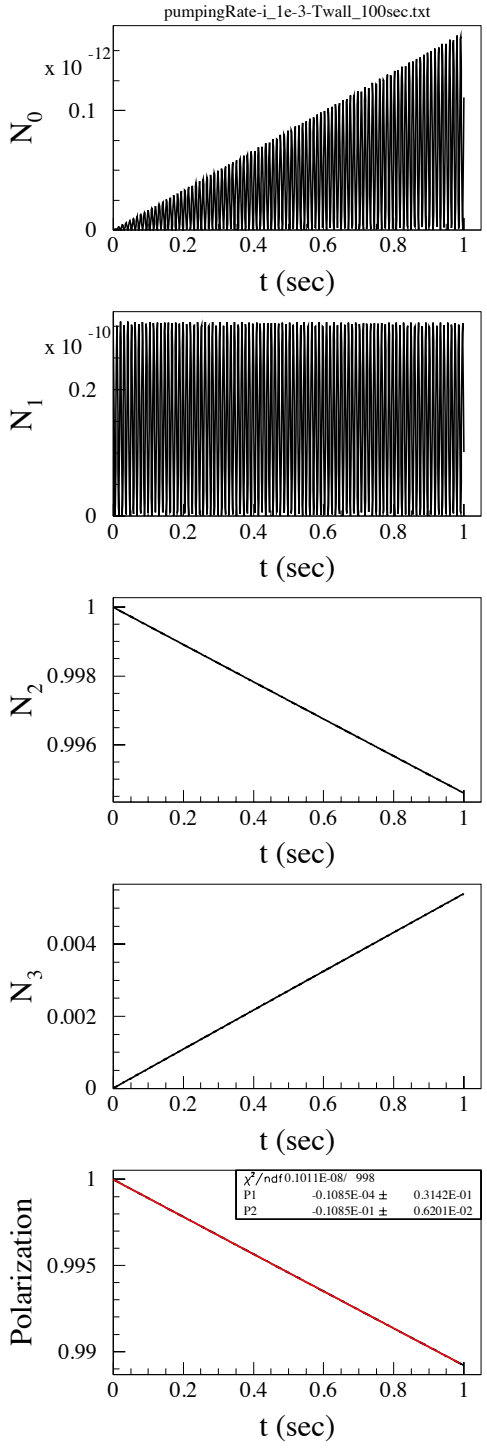

Figure 6: Time evolution of number of density of ^{199}Hg atomic states calculated by the rate equation. The probe light intensity is $I = 1 \times 10^{-3}$ W/cm^{-2}.

the uncertainty of the magnetic field is 3 fT in one Ramsey measurement, $30^2 = 9 \times 10^2$ set measurements should be performed until the uncertainty is reduced less than 0.1 fT. It takes

$$T_{\rm Meas} = 9 \times 10^2 \times 720 \text{ [sec]} = 6.48 \times 10^5 \text{ [sec]} \tag{22}$$

$$= 7.5 \text{ [day]}. \tag{23}$$

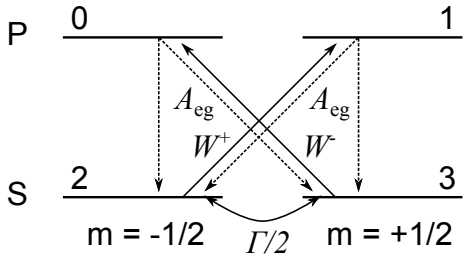

Figure 7: Schematic figure of energy states for ^{199}Hg atom used in the rate equations.

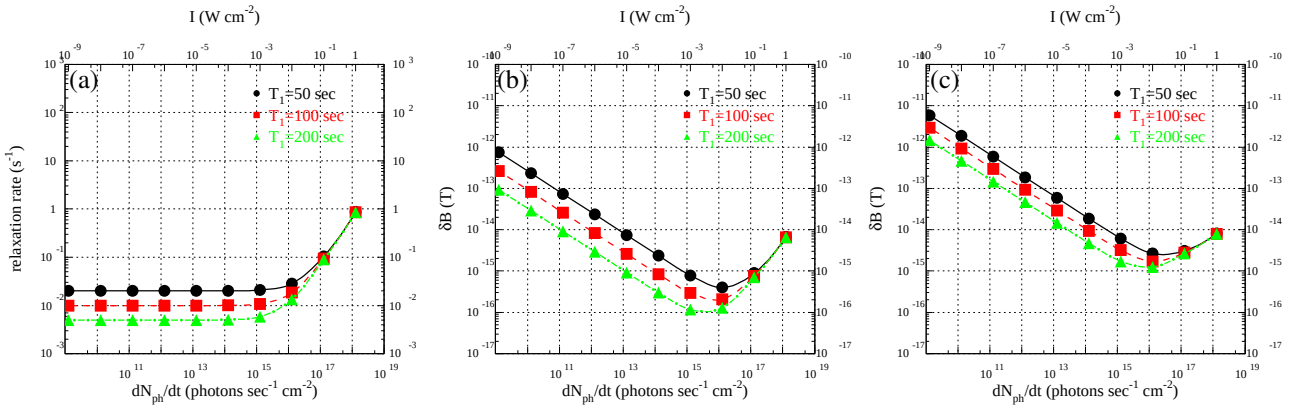

Figure 8: (a):Relaxation rates as a function of photon flux density. (b): Statistical errors obtained by fitting all data during the Ramsey measurement. Vertical axis is statistical errors of the magnetic field and horizontal axis is photon flux density of the probe light. (c) : Statistical errors obtained by using initial and final parts of the Ramsey measurement. Vertical axis is statistical errors of the magnetic field and horizontal axis is photon flux density of the probe light. Here, $n_{\rm cycl} = 2$.

1.3.5 Comparison with Hg EDM experiment

Our co-magnetometer is compared with the Hg atomic EDM experiment [1, 4] in Table 2.

1.4 Systematic error

1.4.1 Light shift

Strong off-resonant radiation causes an apparent shift of the energy levels associated with the optical transition. It is known as light shift. This shift is proportional to the intensity of the light and has a dispersionlike dependence on the optical detuning. Because of their variation from one sublevel to another, the effect of light shifts can be described in terms of fictitious magnetic field [8]. Light shift is cause of systematic errors in the ^{199}Hg magnetometer.

Light shift is expressed in semi-classical form as follows [9, 10],

$$U = \frac{\hbar\Delta}{2}\ln\left[1 + \frac{\chi_0^2/2}{\Delta^2 + (\Gamma/2)^2}\right], \tag{24}$$

where Δ is optical detuning, $\Delta = \omega - \omega_0$ and χ_0 is so-called Rabi frequency and given by

$$\frac{2\chi_0^2}{\Gamma^2} = \frac{I}{I_s}. \tag{25}$$

Here, I, I_s, Γ are light intensity, saturation intensity and decay width, respectively. The saturation intensity is expressed by,

$$I_s = \frac{\pi ch}{3\lambda^3(1/\Gamma)}. \tag{26}$$

T_1 [sec]	I [W/cm^2]	$\delta B_{\text{shot noise}}$ [T]
50	2×10^{-2}	3×10^{-15}
100	1×10^{-2}	2×10^{-15}
200	1×10^{-2}	1×10^{-15}

Table 1: Shot noise limit by the Faraday rotation method.

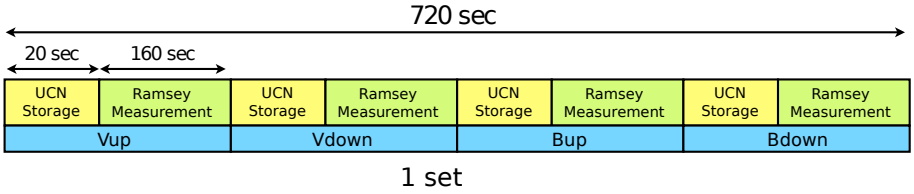

Figure 9: Time scheme of neutron EDM measurement

The saturation intensity, I_s depends on a transition line of an atom. In case of the transition 6^1S_0–6^3P_1 in ^{199}Hg atom [11],

$$I_s = 102\ \text{W/m}^2 = 10.2\ \text{mW/cm}^2, \tag{27}$$

where $\Gamma = 8.00\times10^6\ \text{sec}^{-1}$[12].

When $\Delta \ll \Gamma/2$, $I/I_s \ll 1$,

$$U \sim \frac{\hbar\chi_0^2\Delta}{2\Gamma^2} \tag{28}$$

$$\sim \frac{\hbar\Delta I}{2I_s}. \tag{29}$$

When $\Delta \gg \Gamma/2$, $\Delta \gg \chi_0/\sqrt{2}$,

$$U \sim \frac{\hbar\chi_0^2}{4\Delta} \tag{30}$$

$$\sim \frac{\hbar\Gamma^2 I}{8\Delta I_s}. \tag{31}$$

In the Faraday rotation method, the probe laser frequency is tuned on the midway between the $F = 1/2$ and $3/2$ hyperfine lines; at this frequency, the absorption cross section and light shift is small and circular dichroism is vanished. Here, a detune from the tuned frequency is defined as Δ_M and a frequency difference between the $F = 1/2$ and $F = 3/2$ hyperfine lines is defined as Δ_0. When $\Delta_0/2 \gg \Delta_\text{M}$, light shift in a neighborhood of $\Delta_\text{M} = 0$ is,

$$U = \frac{\hbar\chi_0^2}{4}\left[\frac{1}{\Delta_\text{M} - \Delta_0/2} + \frac{1}{\Delta_\text{M} + \Delta_0/2}\right] \tag{32}$$

$$\sim \frac{\hbar\Gamma^2}{I_s\Delta_0^2} I\Delta_\text{M}. \tag{33}$$

In real condition, Doppler broadening and pressure broadening should be considered. In our experiment, pressure broadening is negligible because the mercury pressure is about saturation pressure. So only the Doppler broadening is considered. With the Doppler broadening function $F_G(\omega)$, light shift is expressed by

$$U(\Delta) = \frac{\hbar}{2}\int_{-\infty}^{\infty}(\Delta - \Delta')\ln\left[1 + \frac{\chi_0^2/2}{(\Delta - \Delta')^2 + (\Gamma/2)^2}\right]F_G(\Delta')d\Delta'. \tag{34}$$

	Hg atom density [cm^{13}]	Cell length [cm]	Faraday rotation angle [mrad]	Absorption coefficient [cm^{-1}]	Probe-light intensity [mW]	Fitting region
Hg-EDM	4×10^{13}	2	600	5×10^{-1}	7×10^{-3}	Entire region
nEDM	3×10^{10}	30	5	6×10^{-8}	1	A few cycles at initial and final

Table 2: Difference of co-magnetometers between the Hg EDM experiment [1, 4] and this nEDM (P33) experiment.

Where the distribution is given by [13],

$$F_G(\omega) = \frac{1}{\sqrt{2\pi\delta^2}} \exp\{-\frac{(\omega-\omega_0)^2}{2\delta^2}\} \tag{35}$$

$$2\Delta_D = 2\omega_0 \sqrt{\frac{2k_BT\ln 2}{Mc^2}} \tag{36}$$

$$\delta = \omega_0 \sqrt{k_BT/Mc^2} = \Delta_D/\sqrt{2\ln 2} \sim \Delta_D/1.18. \tag{37}$$

Here, the wavelengths concerning to the ^{199}Hg magnetometer are shown in Table 3.

Frequency (cm^{-1}) [14]	Wavelength (nm)	F_g	F_e
39 411.946 3	253.730 174	1/2	1/2
39 412.684 7	253.725 421	1/2	3/2

Table 3: The resonance lines for ^{199}Hg atom. F_g, F_e are quantum numbers of total angular moment for ground and excited states, respectively.

The calculated light shift is shown in Fig. 10, where it is assumed that the photon flux density of probe light, $I = 1\times10^2$ W/m^2, and temperature, T =300 K. The gradient of light shift against the flux density is shown in Fig. 11, where detune is about zero.

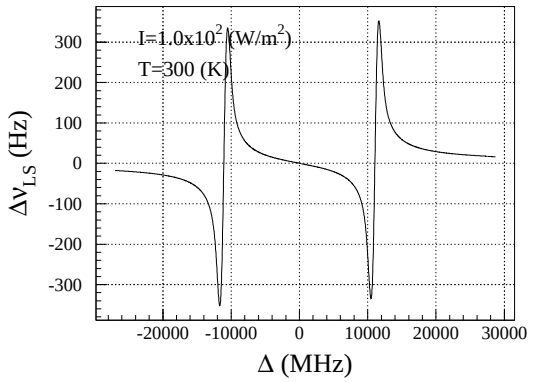

Figure 10: Light shift of ^{199}Hg atoms at T=300 K. (The Doppler broadening is included.)

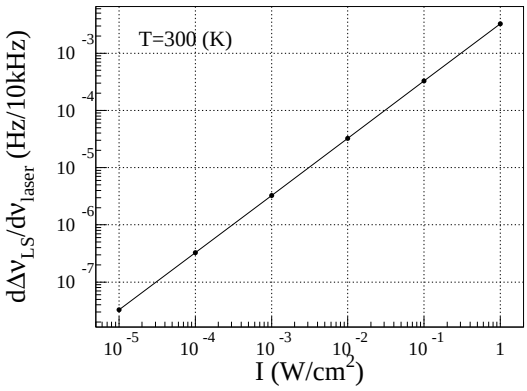

Figure 11: Light shift gradient against light frequency as a function of the photon flux density of the probe light.

1.4.2 Effect of a angular miss-alignment of the probe light and component of circular polarization on light shift

In Eq. (24), it is assumed that the circularly polarized probe light propagates in parallel with quantize axis (direction of $\boldsymbol{B_0}$) as shown in Fig. 12-(a). In the nEDM measurement, the probe light propagates in a direction perpendicular to the direction of $\boldsymbol{B_0}$ (Fig. 12-(b)). So light shift is reduced from the setup shown in Fig. 12-(a).

To estimate the reducing factor, it is assumed that the angular miss-alignment between the B_0 and the direction of the light propagation ($\delta\theta$ indicated in Fig. 12-(b)) and circular polarization, s_3, is assumed as follows,

- $\delta\theta = 1^\circ$
- $s_3 = 4.5{\times}10^{-3}$

The circular polarization is estimated from a extinction ratio achieved by a commercial Glan-Tomson calcite polariser. Light shift is expressed by [15]

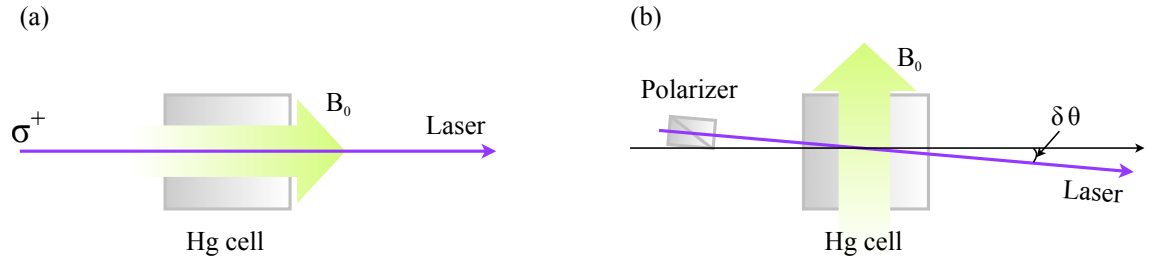

Figure 12: (a): Setup where light shift is maximum. (b): Setup on nEDM (P33) experiment

$$\Delta\nu \propto \nu_V s_3 \cos\theta, \tag{38}$$

where θ is angle between the propagation direction of the probe light and direction of $\boldsymbol{B_0}$. When the propagation direction and quantize axis is aligned as shown in Fig. 12-(b),

$$\cos\theta = \cos(90^\circ \pm \delta\theta) \sim \pm\delta\theta. \tag{39}$$

Substitution of $\delta\theta = 1^\circ$ into the above equation yields

$$\cos\theta \sim \pm 0.017. \tag{40}$$

As the results, measurement uncertainty of the Larmor-frequency of ^{199}Hg atom due to light shift including the miss-alignment and the circular polarization is

$$\delta\nu_{LS} = 2\sqrt{\xi}\cdot\delta\theta\cdot\Delta\nu_{LS0}. \tag{41}$$

Here, $\Delta\nu_{LS0}$ is light shift when circular polarized light is incident in parallel with magnetic field $\boldsymbol{B_0}$.

1.4.3 Acceptable fluctuation on frequency of probe light

Gradients of $\delta\nu_{\mathrm{LS}}$ in Eq. (41) against optical detune as a function of photon flux density are shown in Fig. 13. When $\Delta \sim 0$, light shift can be approximated with Eq.(33) and the photon flux density of the probe light, I and frequency fluctuation of the probe light, $\delta\nu_{\mathrm{laser}}$ around $\Delta \sim 0$ is expressed by

$$I\delta\nu_{\mathrm{laser}} = \frac{\delta\nu_{\mathrm{Hg}}}{a}. \tag{42}$$

Where $\delta\nu_{\mathrm{Hg}}$ is aiming measurement accuracy of Larmor frequency and a is constant. Fitting result in Fig. 13 shows

$$a = 2.4\times10^{-7}\ \mathrm{Hz}\cdot(10\ \mathrm{kHz})^{-1}\cdot\mathrm{W}^{-1}\cdot\mathrm{cm}^2 \tag{43}$$

$$= 2.4\times10^{-8}\ \mathrm{W}^{-1}\cdot\mathrm{cm}^2. \tag{44}$$

The relationships for $\delta\nu_{\mathrm{Hg}} = 1{\times}10^{-8}$ Hz (dot-dashed line), $1{\times}10^{-9}$ Hz(dashed line) and $1{\times}10^{-10}$ Hz(solid line) are shown in Fig. 14. Requirements for the probe light is lower-left region of each line in Fig. 13. For example, when $\delta\nu_{\mathrm{Hg}} = 1\times10^{-9}$ Hz and $I = 1\times10^{-3}$ W/cm^2, it is necessary to keep the frequency fluctuation lower than 40 kHz.

The relationship between uncertainty of magnetic field δB and that of Larmor frequency is expressed as follows,

$$\gamma\delta B = \delta\omega \tag{45}$$

$$\gamma = 0.4770\times10^8\ \mathrm{s}^{-1}\mathrm{T}^{-1} \tag{46}$$

$$\delta\omega = 2\pi\delta\nu_{\mathrm{Hg}}. \tag{47}$$

And when $\delta B = 0.1$ fT,

$$\delta\nu_{\mathrm{Hg}} = 0.4770\times10^8\times0.1\times10^{-15}/(2\pi), \tag{48}$$

$$= 0.759\times10^{-9}\ \mathrm{Hz}. \tag{49}$$

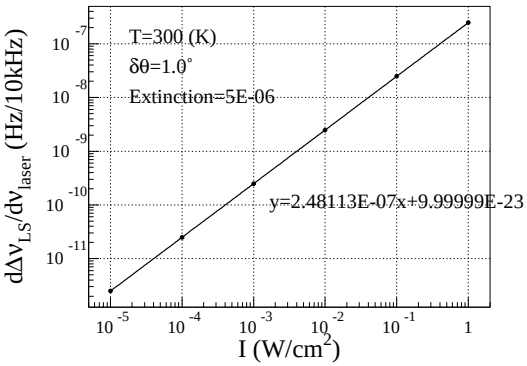

Figure 13: Behavior of light shift gradient against frequency of probe light as a function of the photon flux density, where $\delta\theta = 1^\circ$ and extinction ratio of the polariser is 5×10^{-6}.

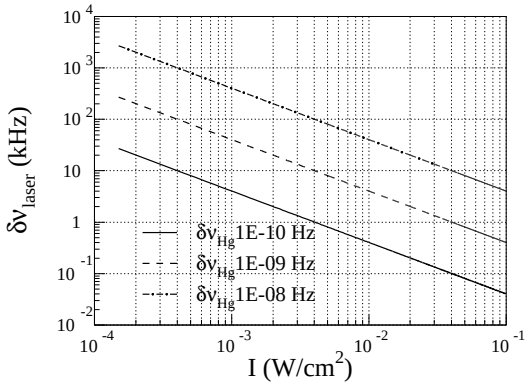

Figure 14: Acceptable intensity fluctuation $\delta\nu_{\rm laser}$ as a function of the photon flux density (I). Each line is different in aiming measurement accuracy of ^{199}Hg Larmor frequency ($\delta\nu_{\rm Hg}$).

1.4.4 Measurement accuracy of magnetic field when intensity of probe light is fluctuated

Equation (33) shows that light shift is linear function of optical detune Δ and light intensity I. Assume the proportional constant is A,

$$\delta\nu_{\rm LS}(I,\Delta) = AI\Delta. \tag{50}$$

Upon differentiating the above equation by I, we therefore have

$$\frac{d\delta\nu_{\rm LS}}{dI} = A\Delta. \tag{51}$$

In Fig. 15, light shift is plotted as a function of the photon flux density of the probe light, where $\Delta \gg \Delta_{\rm M}$ (Δ =24 MHz). Upon fitting this graph with a linear function, following result are obtained,

$$\left.\frac{d\Delta\nu_{LS}}{dI}\right|_{\Delta=24MHz} = 6.0\times10^{-4}\ \text{Hz}\cdot\text{W}^{-1}\cdot\text{cm}^2, \tag{52}$$

$$= A\Delta, \tag{53}$$

$$A = 2.5\times10^{-11}\ \text{W}^{-1}\cdot\text{cm}^2. \tag{54}$$

In general, Eq (50) is expressed by

$$\delta\nu_{\rm Hg} = AI\delta_R\delta\nu_{\rm laser}, \tag{55}$$

here, $\delta\nu_{\rm Hg}$, $\delta\nu_{\rm laser}$, and $\delta_R(=\delta I/I)$ are a target measurement accuracy of Larmor frequency for ^{199}Hg, an allowable frequency deviation from the aiming line (midway between $F = 1/2$ and $F = 3/2$) of the probe light, and allowable intensity variation, respectively.

Substitution of $I = 1\times10^{-3}$ W/cm^2 into Eq. 55 yields

$$\delta_R\delta\nu_{\rm laser} = \frac{\delta\nu_{\rm Hg}}{AI} \tag{56}$$

$$= 4.0\times10^{13}\cdot\delta\nu_{\rm Hg}\ [\text{Hz}]. \tag{57}$$

For example, if the intensity of the probe light is fluctuated by 3% [16], a required accuracy of absolute frequency to achieve the frequency accuracy of 1 nHz is

$$\text{(Absolute accuracy of frequency)} = 4.0\times10^{13}\times1\times10^{-9}/0.03\ \text{Hz} \tag{58}$$

$$= 1.3\ \text{MHz}. \tag{59}$$

A relationship between Δ_R and $\Delta\nu_{\rm laser}$ in Eq.(57) are plotted in Fig. 16. Where, the solid, dashed, and dot-dashed line are calculations at aiming accuracy of frequency measurement $\delta_{\rm Hg}$ of 1×10^{10} Hz, 1×10^{-9} Hz, and 1×10^{-8} Hz, respectively. The allowable region is lower left one for each line.

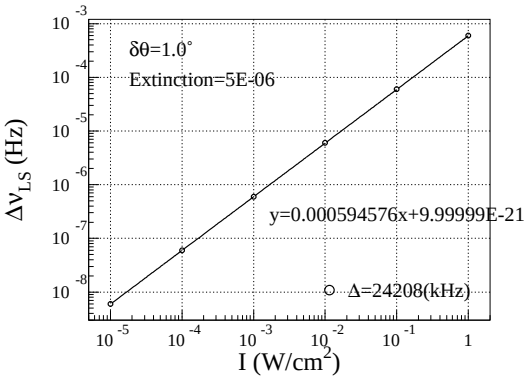

Figure 15: Light shift as a function of the photon flux density at $\Delta = 24$ MHz where the approximation in Eq. (57) can be used.

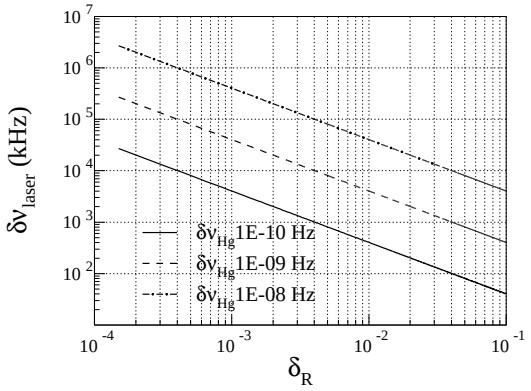

Figure 16: The intensity fluctuation (δ_R) vs uncertainty of the absolute frequency of the probe light ($\delta\nu_{\text{laser}}$). Each line is different in the aiming measurement uncertainty of the Larmor frequency of ^{199}Hg atom, $\delta\nu_{\text{Hg}}$.

1.5 Summary for Faraday-rotation method

- The shot-noise limit in a Ramsey measurement is 3 fT; where the relaxation time of the ^{199}Hg atom (T_1) of 100 sec and the photon flux density (I) of 1×10^{-3} W/cm^2 are assumed. It takes 7.5 days to decrease this lower than 0.1 fT.
- Following performances are required for the probe light laser to decrease systematic errors caused by light shift less than 1 nHz.
  - The photon flux density: 1×10^{-3} mW/cm^2
  - Relative frequency fluctuation: < 40 kHz
  - Uncertainty of absolute frequency: < 1.3 MHz
  - Fluctuation of light intensity <3%

2 Absorption method

2.1 Measurement Scheme

A measurement scheme of the absorption method is shown in Fig. 17. In this method, circular polarized photon whose frequency is coincide with absorption line of ^{199}Hg atom are transmitted through the ^{199}Hg cell; where the ^{199}Hg atoms are precessing around a quantization (B_0) axis. The transmitted light intensity is modulated at frequency of the Larmor precession. The magnetic field can be obtained by the modulation frequency.

2.2 Statistical error: Shot noise

By the same method described at section 1.3.3, the relaxation of polarization is estimated. Absorption coefficient as a function of photon frequency is shown in Fig. 18 (refer to Appendix C). From this figure, the absorption cross section is derived as follows.

$$\sigma_{\text{abs}} = \alpha_\nu(\Delta f = 0)/n_{\text{g}} \tag{60}$$

$$= 3.7 \times 10^{-13}\ [\text{cm}^2]. \tag{61}$$

Upon substituting this value into Eq. (21), the rate equations (12)-(15) are numerically calculated. In Fig. 19-(a), relaxation rates as a function of the photon flux density of probe light are plotted. From this result, shot noise limit is obtained as a function of the flux density in Fig. 19-(b) and -(c). Figure 19-(c) is the shot noise calculated by using Eq. (2). When a relaxation time $T_1 = 100$ sec, the minimum value of δB is obtained at the flux density of 1×10^{-7} W/cm^2, and it is 5×10^{-14} T.

The shot noise limits of the magnetic field measurement obtained from Fig. 19-(c) are summarized in table. 4 for each T_1.

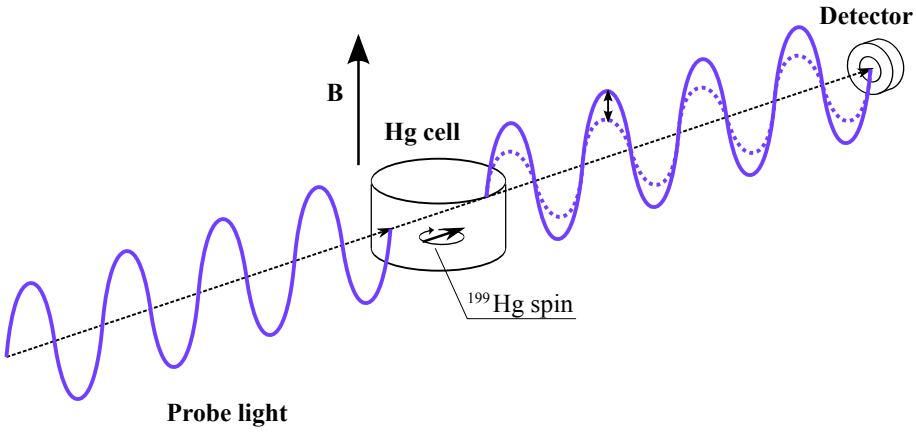

Figure 17: Setup for the absorption method

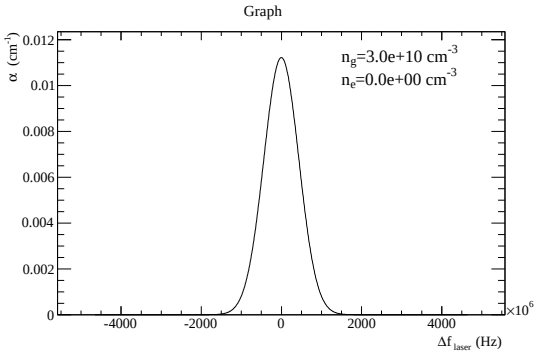

Figure 18: Absorption coefficient (α_ν)

Since the shot noise at $T_1 = 100$ sec is 5×10^{-14} T, it is necessary to reduce the statistical error by 1/500 to achieve the uncertainty of less than 0.1 fT. To do this, we need $500^2 = 2.5 \times 10^5$-set Ramsey measurements according to discussion described in section 1. So it takes

$$T_{\text{Meas}} = 2.5 \times 10^5 \times 720 \text{ [sec]} = 1.8 \times 10^8 \text{ [sec]} \tag{62}$$

$$= 2083 \text{ [day]}. \tag{63}$$

This time is very long and is not practical.

2.3 Systematic error: Light shift

2.3.1 Allowable relative frequency-fluctuation of the probe light

In Fig. 20, light shift is plotted as a function of detune, Δ, where the photon flux density (I), temperature (T) are 1×10^{-3} W/m^2, 300 K, respectively. Fig. 21 shows gradient of light shift against the detune as a function of I.

This is light shift where the circularly polarized probe light in direction of quantize axis ($\boldsymbol{B_0}$). In Fig. 22, the gradients of light shift is plotted as a function of the photon flux density, where the probe light propagates along deviated axis from perpendicular direction of the quantize axis by $1^c irc$. This figure is obtained by scaling the vertical axis in Fig. 11 by 0.017.

From Eq. (29), the relationship between the photon flux density,I and relative frequency-fluctuation of the probe light, $\delta\nu_{\text{laser}}$ can be obtained as follows in a neighborhood of $\Delta = 0$,

$$I\delta\nu_{\text{laser}} = \frac{\delta\nu_{\text{Hg}}}{a}, \tag{64}$$

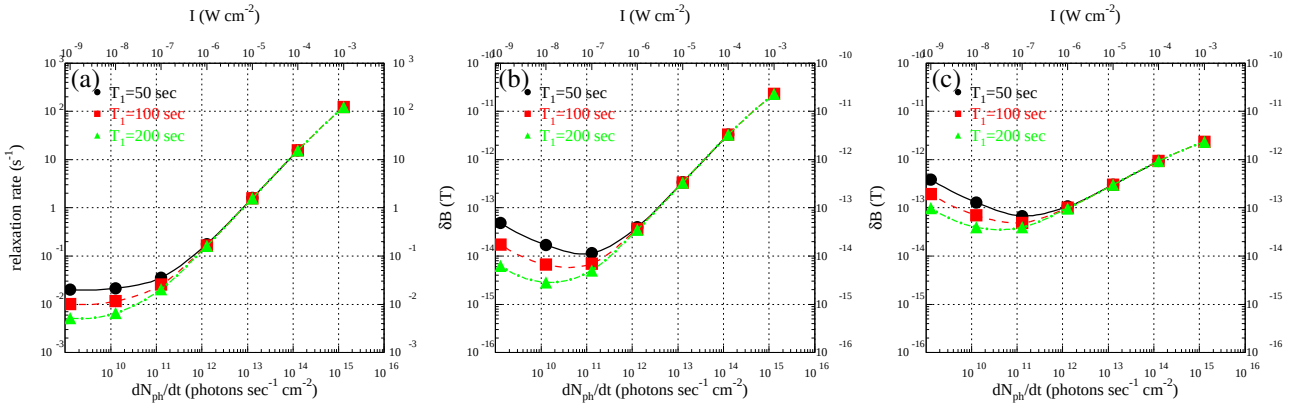

Figure 19: (a) Relaxation time of ^{199}Hg as a function of the photon flux density of the probe light. (b) Shot noise when the frequency is determined by fitting entire span within one Ramsey measurement. (c)Shot noise when the frequency is determined by fitting first two cycle of the Larmor period and final two cycle one; $n_{\rm cycl} = 2$ in Eq. 2.

T_1 [sec]	I [W/cm^2]	$\delta B_{\rm shot\ noise}$ [T]
50	2×10^{-7}	7×10^{-14}
100	1×10^{-7}	5×10^{-14}
200	3×10^{-8}	4×10^{-14}

Table 4: Shot noise limits in the absorption method when the frequency determined with initial and final phase.

where a is a constant. From Fig. 22,

$$a = 0.0159\ \text{Hz} \cdot (10\ \text{kHz})^{-1} \cdot \text{W}^{-1} \cdot \text{cm}^2 \tag{65}$$
$$= 0.00159\ \text{W}^{-1} \cdot \text{cm}^2 \tag{66}$$

is obtained. By substituting above equation into Eq. (64), the relationship between the photon flux of the probe light and allowable frequency fluctuation are obtained and is plotted in Fig. 23; where solid, dashed, and dot-dashed lines indicates for the target accuracy, $\delta\nu_{\rm Hg}$ of 1×10^{-10}, 1×10^{-9} 1×10^{-8} Hz, respectively. For example, when $\delta\nu_{\rm Hg} < 1 \times 10^{-9}$ Hz and $I = 1 \times 10^{-7}$ W/cm^{-2}, the relative frequency-fluctuation of the probe light should be less than 6 kHz.

2.3.2 Allowable uncertainty of absolute frequency for probe-light and intensity fluctuation

In Fig. 24, light shift, $\delta\nu_{\rm LS}$, of ^{199}Hg atom is shown as a function of the photon flux density when $\Delta = 7.8$ MHz; where light shift U can be approximated with Eq. 29. The fitting by a first order polynomial function yields,

$$\left.\frac{d\delta\nu_{\rm LS}}{dI}\right|_{\Delta=7.8MHz} = 23\ \text{Hz}\cdot\text{W}^{-1}\cdot\text{cm}^2. \tag{67}$$

With the same procedure as described in section 1.4.4, the constant A is obtained by

$$A = \frac{23}{7.8 \times 10^6} = 3.0 \times 10^{-6}. \tag{68}$$

Suppose $I = 1 \times 10^{-7}$ W/cm^2, the relationship between δ_R and $\delta\nu_{\rm laser}$ becomes

$$\delta_R \delta\nu_{\rm laser} = \frac{\delta\nu_{\rm Hg}}{AI} \tag{69}$$
$$= 0.33 \times 10^{13} \cdot \delta\nu_{\rm Hg}\ [\text{Hz}]. \tag{70}$$

If $\delta_R = 3$ % [16], the absolute accuracy of the probe-light frequency to achieve the measurement uncertainty of the Larmor frequency, $\delta\nu_{\rm Hg} = 1 \times 10^{-9}$ Hz is

$$\delta\nu_{\rm laser} = 0.33 \times 10^{13} \times 1 \times 10^{-9}/0.03\ \text{Hz} \tag{71}$$
$$= 0.11\text{MHz}. \tag{72}$$

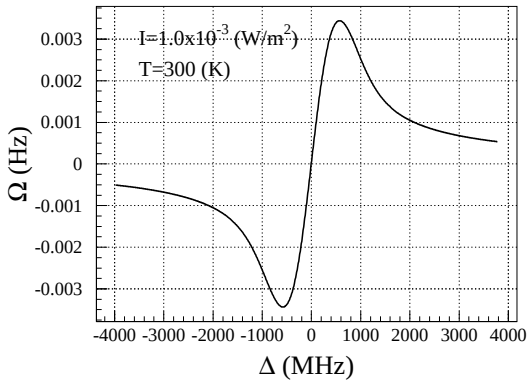

Figure 20: Light shift of ^{199}Hg atom; where atomic vapor temperature is 300 K.

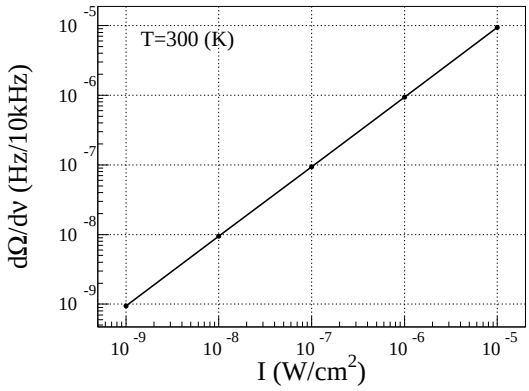

Figure 21: Light shift gradient against the detune as a function of the photon flux density.

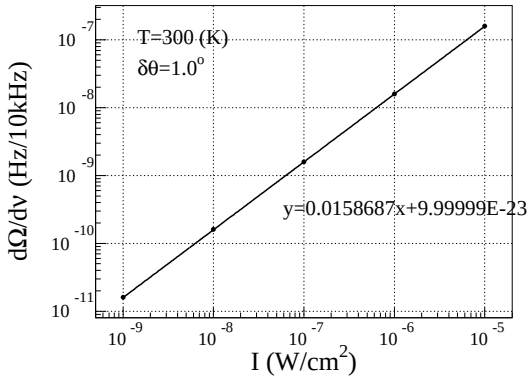

Figure 22: The gradients of light shift against the frequency of the probe light as a function of the photon flux density of the probe light, where the light propagates in direction deviate from the perpendicular direction with respect to quantize axis of B_0.

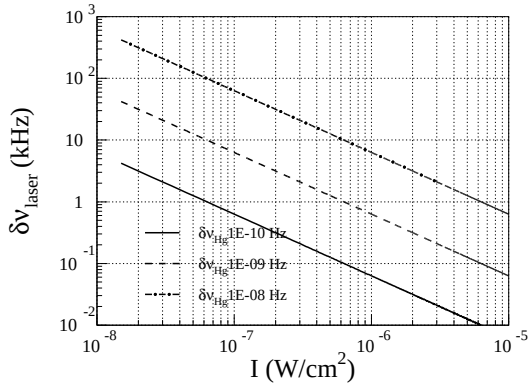

Figure 23: The intensity fluctuation (δ_R) vs uncertainty of the absolute frequency of the probe light ($\delta\nu_{\rm laser}$). Each line is different in the aiming measurement uncertainty of the Larmor frequency of ^{199}Hg atom, $\delta\nu_{\rm Hg}$.

2.4 Summary of absorption method

- To achieve systematic error caused by light shift less than 1 nHz, the probe light is required to meet following performances.
  - Photon flux density: $< 1 \times 10^{-7}$ W/cm^2
  - Relative frequency fluctuation: < 6 kHz
  - Absolute accuracy of frequency: < 0.11 MHz
  - Intensity fluctuation: <3%
- In one Ramsey measurement, shot noise of this magnetometer is 5×10^{-14} T upon supposing the relaxation time T_1 of 100 sec. It takes 2000 days to reduce the shot noise less than 0.1 T.

3 Summary

The accuracy of the mercury magnetometer used as co-magnetometer of nEDM measurement were estimated for two methods, the Faraday rotation method and the absorption method. They are summarized in Table 5. The absorption method can not achieve the aiming accuracy of 0.1 fT due to the shot-noise limit, on the other hand, the Faraday rotation method is feasible. In the Faraday rotation method, it is required to use a high-intense (more than 1 mW) tunable UV laser as the probe laser and such laser is commercially available. The required accuracy of relative and absolute frequency is not guaranteed by a fabrication maker, however such requirements have been achieved in laboratory level [17].

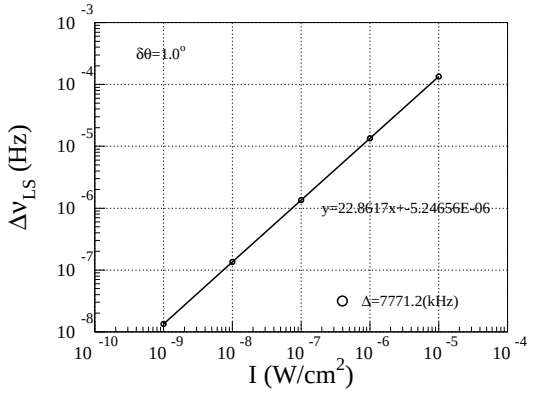

Figure 24: Light shift as a function of the photon flux density at $\Delta = 7.8$MHz.

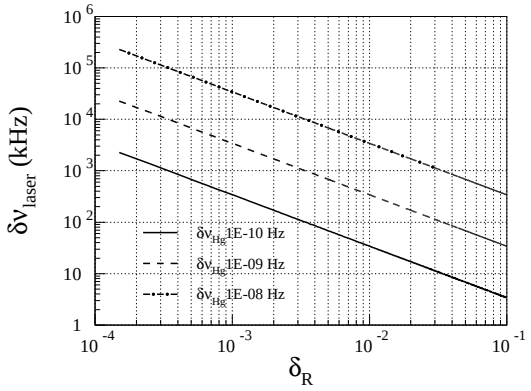

Figure 25: The absolute-frequency accuracy of the probe light as a function of the intensity fluctuation of the probe light.

	Faraday rotation method	Absorption method
Photon flux density	1×10^{-3} W/cm^2	1×10^{-7} W/cm^2
Allowable relative frequency-fluctuation	< 40 kHz	< 6 kHz
Allowable uncertainty of absolute frequency	< 1.3 MHz	< 0.11 MHz
Allowable intensity fluctuation	<3%	<3%
Measurement time	8 days	2000 days

Table 5: Required performance for the Faraday rotation method and the absorption method and required measurement time to achieve field uncertainty less than 0.1 fT.

A Energy level of mercury

The energy level related to the ^{199}Hg magnetometer is shown in Fig. 26.

B Analytical form of shot noise

To derive analytical forms of shot noise, a simplified model is used as follows,

- During Larmor precession period, the polarization is constant before relaxation ($t < T_1$). After the relaxation is occurred, the polarization become zero ($t > T_1$).
- Measurement data on amplitude center of sinusoidal signal are only used.
- Error in direction of time is ignored.

B.1 Entire fitting of Ramsey measurement

If the magnetic field does not fluctuate during a Ramsey measurement, the Larmor frequency can be obtained by fitting a entire region of the measurement. Here it is supposed to fit signals of the transmitted light with a least square method. In the mercury magnetometer, the obtained signal is expressed by

$$I(t) = I_0 \sin(\omega t + \phi) + I_c, \tag{73}$$

where fitting parameter is ω. This function is converted to the phase advance as a function of time as follows,

$$\phi_i(t) = \omega_0 t_i + \phi_0, \tag{74}$$

where ω_0, ϕ_0 are fitted values of ω, ϕ in Eq (73), respectively.

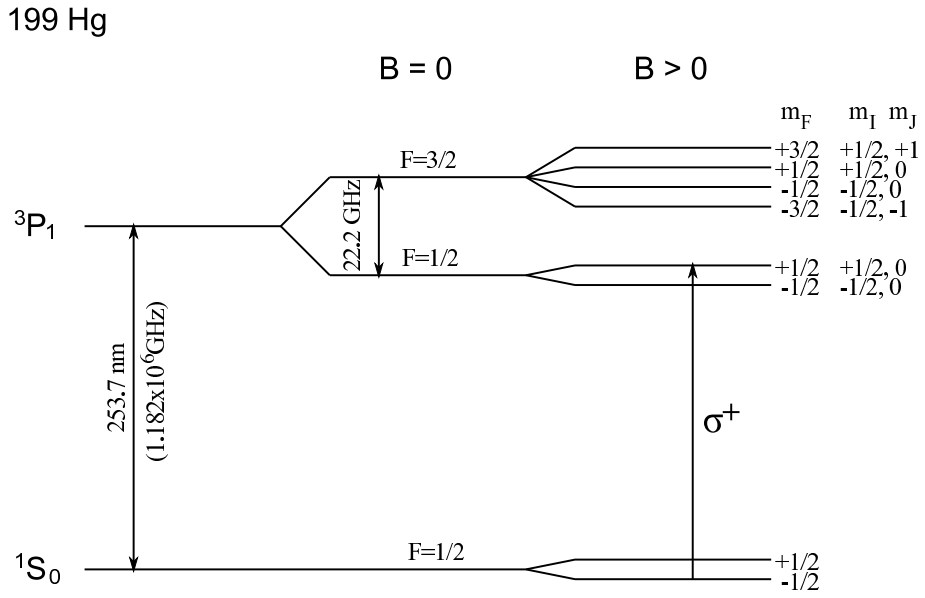

Figure 26: Energy level of Mercury 199 related to the Hg magnetometer

The error of the fitted parameter, $\delta\omega_0$ is given by

$$(\delta\omega)^2 = \frac{N(\delta\phi)^2}{\Delta}, \tag{75}$$

where $\delta\phi$, N are an error of the ϕ_0 and number of cycles of the Larmor precession observed in the signals of the transmitted light. And Δ is expressed by

$$\Delta = N\sum_1^N t_i^2 - \left(\sum_1^N t_i\right)^2, \tag{76}$$

$$= \frac{N\pi^2}{\omega^2}\frac{N(N+1)(2N+1)}{6} - \frac{\pi^2}{\omega^2}\frac{N^2(N+1)^2}{4}, \tag{77}$$

$$= \frac{N^2\pi^2}{12\omega^2}\left(N^2-1\right), \tag{78}$$

where

$$N = \omega T_0/2\pi, \tag{79}$$

$$t_n = n\pi/\omega, \tag{80}$$

were used, here n is integer more than 0. When $\omega t + \phi \sim 0$, from Eq. (73)

$$\delta\phi = \frac{\delta I}{I_0}. \tag{81}$$

Substation of Eq. (78) and (81) into Eq. (75) yields

$$(\delta\omega)^2 = \frac{12\omega^2}{\pi^2 N(N^2-1)}\left(\frac{\delta I}{I_0}\right)^2. \tag{82}$$

Since $N \gg 1$, above equation is approximated as

$$(\delta\omega)^2 \sim \frac{12\omega^2}{\pi^2 N^3}\left(\frac{\delta I}{I_0}\right)^2, \tag{83}$$

$$\sim \frac{12\pi}{\omega T_0^3}\left(\frac{\delta I}{I_0}\right)^2. \tag{84}$$

Where Eq. (79) was used.

By using a following equation,

$$\omega = \gamma B, \tag{85}$$

Eq. (84) can be rewritten as

$$\delta B = \frac{\delta\omega}{\gamma} \tag{86}$$

$$= \frac{\sqrt{12\pi}}{\gamma\sqrt{\omega T_0^3}}\frac{\delta I}{I_0}. \tag{87}$$

By using following equation,

$$\alpha = I_0/I_c, \tag{88}$$

$$0 < \alpha \leq 1, \tag{89}$$

Eq. (73) is changed to

$$I(t) = I_c(\alpha\sin(\omega t + \phi) + 1). \tag{90}$$

Here, since it is assumed that $\omega t + \phi \sim n\pi/2$ for the fitting data and δI is statistical errors,

$$I \sim I_c, \tag{91}$$

$$\delta I = \sqrt{I} \sim \sqrt{I_c}. \tag{92}$$

Substitution of above equations into Eq. (87)yields

$$\delta B = \frac{\sqrt{12\pi}}{\alpha\gamma\sqrt{\omega T_0^3}}\frac{\sqrt{I_c}}{I_c}. \tag{93}$$

Where I_c, I_0 are expressed by

$$I_c = \dot{N}_{\mathrm{phc}}\Delta t, \tag{94}$$

$$I_0 = \dot{N}_{\mathrm{ph0}}\Delta t, \tag{95}$$

$$= \alpha\dot{N}_{\mathrm{phc}}\Delta t, \tag{96}$$

here $\dot{N}_{\mathrm{phc}}$ and $\dot{N}_{\mathrm{ph0}}$ is the number of photon per unit time and Δt is bin width of measurement time. If it is set to $\Delta t = \pi/(2\omega)$, following equation can be obtained,

$$I_c = \pi\dot{N}_{\mathrm{phc}}/(2\omega), \tag{97}$$

$$\delta I_c = \sqrt{\pi\dot{N}_{\mathrm{phc}}/(2\omega)}. \tag{98}$$

As the results the following equation is obtained,

$$\delta B = \frac{2\sqrt{6}}{\alpha\gamma\sqrt{T_0^3\dot{N}_{\mathrm{phc}}}}. \tag{99}$$

B.2 In case to obtain the Larmor frequency by fitting of a few initial cycles and final cycles during Ramsey measurement period

In the Ramsey measurement, integrated angle of the Larmor precession is measured, where the neutron is pressing during 150 sec. It is possible that the magnetic field is fluctuated during the measurement time due to small disturbance field from unknown external sources. In such a case, the integrated angle during the measurement is obtained from a phase

difference between initial phase of the Larmor precession of ^{199}Hg atoms and final one; these phases are obtained by fitting a few cycle data of an initial and final Larmor-precession signal in the Ramsey measurement. The statistical error is calculated as follows [18].

$$\sigma_f^2 = \frac{2}{\pi^2}\frac{1}{\alpha^2 N_{\rm cs}}\frac{1}{T_0^2} \tag{100}$$

Here, ω_L, $N_{\rm cs}$ are the Larmor angular frequency of the ^{199}Hg and photon counts in the fitting region. When the number of cycle for initial and final one is $n_{\rm cycl}$ for each, $N_{\rm cs}$ is expressed by

$$N_{\rm cs} = \dot{N}_{\rm ph} t_s \tag{101}$$
$$= \dot{N}_{\rm ph} 2\pi n_{\rm cycl}/\omega_L. \tag{102}$$

Substitution of Eq. 101 into the Eq. 100 yields

$$\sigma_f^2 = \frac{\omega_L}{\pi^3 n_{\rm cycl}\alpha^2 \dot{N}_{\rm ph} T_0^2} \tag{103}$$
$$\sigma_f = \sqrt{\frac{\omega_L}{\pi^3 n_{\rm cycl}\alpha^2 \dot{N}_{\rm ph}}}\frac{1}{T_0}. \tag{104}$$

The above equation is reduced to the field uncertainty as follows,

$$\delta B = 2\pi\sigma_f/\gamma \tag{105}$$
$$= \frac{2}{\alpha\gamma}\sqrt{\frac{\omega_L}{\pi n_{\rm cycl}\dot{N}_{\rm ph}}}\frac{1}{T_0}. \tag{106}$$

C Photo absorption cross section of the mercury atom

Transmittance of the medium T_ν is expressed as follows,

$$T_\nu = \exp(-\alpha_\nu L). \tag{107}$$

Here, α is absorption coefficient and given by[14],

$$\alpha_\nu = K_{\rm eg} G(\nu) \tag{108}$$
$$K_{\rm eg} = \frac{\lambda_{\rm eg}^2 A_{\rm eg}}{8\pi c}\left(\frac{g_e}{g_g} n_G - n_E\right) \tag{109}$$
$$= \frac{\lambda_{\rm eg}^2 A_{\rm eg}}{8\pi c}\left(n_g - n_e\right) g_e \tag{110}$$
$$G(\nu) = \frac{2\sqrt{\ln 2}}{\sqrt{\pi}\Delta\nu_D}\exp\left[-\frac{4\ln 2(\nu-\nu_0)}{\Delta\nu_D^2}\right], \tag{111}$$

where n_g, n_e are atomic number density of ground state and excited state, respectively and n_G, n_E are population density of f ground state and excited state, respectively and g_g, g_e are the ground and excited state degeneracies, respectively, and are expressed by

$$g_g = 2F_g + 1 \tag{112}$$
$$g_e = 2F_e + 1. \tag{113}$$

Then, n_g and n_e is given by [19],

$$n_g = \frac{n_G}{2F_g + 1} \tag{114}$$
$$n_e = \frac{n_E}{2F_e + 1}. \tag{115}$$

When there are two resonance line, the absorption coefficient becomes

$$\alpha_\nu = \alpha_\nu^{(F_1)} + \alpha_\nu^{(F_2)}. \tag{116}$$

Calculated absorption coefficient for ^{199}Hg atom is shown in Fig. 27; where two hyperfine lines to $F = 1/2$ and $F = 3/2$ from the ground state are included. Set a frequency of incident light = (center of $F = 1/2$ and $F = 3/2$), the absorption length is

$$\alpha_\nu = 6 \times 10^{-8}\ \mathrm{cm}^{-1}, \tag{117}$$

where atomic density of the ^{199}Hg is $N = 3.0 \times 10^{10}$ atoms/cm^3.

The absorption cross section is

$$\sigma_{\mathrm{phot}} = 2 \times 10^{-18}\ \mathrm{cm}^2. \tag{118}$$

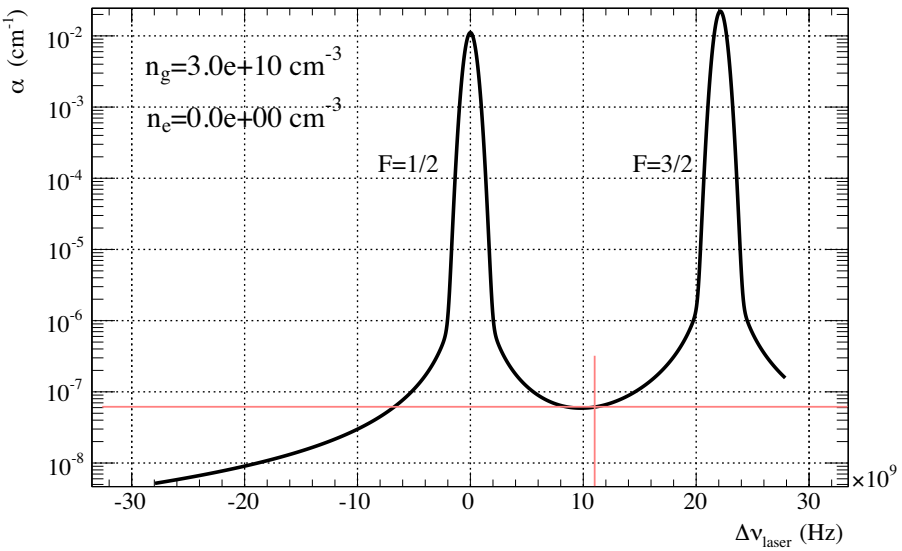

Figure 27: Photo absorption coefficient for ^{199}Hg atom including two resonance, 6^1S_0-$6^3P_1(F{=}1/2)$ 6^1S_0-$6^3P_1(F{=}3/2)$; where number density of the ^{199}Hg atoms is $N = 3.0 \times 10^{10}$ atoms/cm^3.

D Faraday rotation

The Faraday rotation angle is expressed by [20],

$$\phi = \frac{\omega L}{2c}(n_+ - n_-). \tag{119}$$

Here, ω is angular frequency of the probe light, L is length of a medium, c is light speed, and n_+, n_- are refractive index for two counter-rotating circular components, σ^+ and σ^- of the probe light.

また The electric dipole moment μ_e can be written as

$$\mu_{\mathrm{e}}^2 = \frac{e^2\sigma_0\Gamma}{8\pi\alpha_{\mathrm{f}}\omega_0} \tag{120}$$

where α_{f} is the fine structure constant, e is the charge of an electron. σ_0 is photo absorption cross section of ^{199}Hg atom and

$$\sigma_0 \equiv 6\pi\left(\frac{c}{\omega_0}\right)^2. \tag{121}$$

Γ is the natural full line width of the transition in angular frequency and for Hg atom [12],

$$\Gamma_{\mathrm{Hg}} = 8.00 \times 10^6 \ \mathrm{s}^{-1}. \tag{122}$$

The refractive index is expressed by [20],

$$n_{\pm} = 1 + \frac{2\pi\alpha_{\mathrm{f}} c \mu_{\mathrm{e}}^2}{e^2}\left(g^{(3/2)}N_{\pm 1/2} + \frac{2}{3}g^{(1/2)}N_{\mp 1/2} + \frac{1}{3}g^{(3/2)}N_{\mp 1/2}\right), \tag{123}$$

where $g(F')$ is the dispersive function at the center frequency $\omega(F')$, which is the resonance frequency between the ground and each hyperfine excited state F', and $N_{\pm 1/2}$ is the number density of atoms in the ground state $m_I = \pm 1/2$, respectively. Dispersive function, g is given by

$$g_{mj'} = \frac{\omega_{mj'} - \omega}{(\omega_{mj'} - \omega)^2 + (\Gamma/2)^2}. \tag{124}$$

References

[1] W. C. Griffith, M. D. Swallows, T. H. Loftus, M. V. Romalis, B. R. Heckel, E. N. Fortson, Improved limit on the permanent electric dipole moment of ^{199}Hg, Phys. Rev. Lett. 102 (2009) 101601.

[2] K. Green, P. G. Harris, P. Iaydjiev, D. J. R. May, J. M. Pendlebury, K. F. Smith, M. van der Grinten, P. Geltenbort, S. Ivanov, Performance of an atomic mercury magnetometer in the neutron edm experiment, Nucl. Instrum. and Meth. A 404 (2-3) (1998) 381–393. doi:10.1016/S0168-9002(97)01121-2.

[3] C. A. Baker, D. D. Doyle, P. Geltenbort, K. Green, M. G. D. van der Grinten, P. G. Harris, P. Iaydjiev, S. N. Ivanov, D. J. R. May, J. M. Pendlebury, J. D. Richardson, D. Shiers, K. F. Smith, Improved experimental limit on the electric dipole moment of the neutron, Phys. Rev. Lett. 97 (13) (2006) 131801. doi:10.1103/PhysRevLett.97.131801.

[4] B. Heckel, New results from a search for the permanent electric dipole moment (EDM) of ^{199}Hg, in: Presentation at The 4th International Workshop "From Parity Violation to Hadronic Structure and more...", Bar Harbor, Maine, USA, 2009.
URL http://web.mit.edu/pavi09/speakerlist.html

[5] D. Budker, W. Gawlik, D. F. Kimball, S. M. Rochester, V. V. Yashchuk, A. Weis, Resonant nonlinear magneto-optical effects in atoms, Rev. Mod. Phys. 74 (4) (2002) 1153–1201. doi:10.1103/RevModPhys.74.1153.

[6] D. Tupa, L. W. Anderson, Effect of radiation trapping on the polarization of an optically pumped alkali-metal vapor in a weak magnetic field, Phys. Rev. A 36 (5) (1987) 2142–2147. doi:10.1103/PhysRevA.36.2142.

[7] A. Yariv, Optical Electronics in Modern Communications, 5th Edition, Maruzen Co., LTD., 2000.

[8] C. Cohen-Tannoudji, J. Dupont-Roc, Experimental study of zeeman light shifts in weak magnetic fields, Phys. Rev. A 5 (2) (1972) 968–984. doi:10.1103/PhysRevA.5.968.

[9] S. Stenholm, Laser cooling and trapping, European Journal of Physics 9 (4) (1988) 242. doi:10.1088/0143-0807/9/4/001.
URL http://stacks.iop.org/0143-0807/9/i=4/a=001

[10] V. I. Balykin, V. G. Minogin, V. S. Letokhov, Electromagnetic trapping of cold atoms, Reports on Progress in Physics 63 (9) (2000) 1429. doi:10.1088/0034-4885/63/9/202.
URL http://stacks.iop.org/0034-4885/63/i=9/a=202

[11] T. Walther, Prospects of trapping neutral mercury, J. Mod. Opt. 54 (2007) 2523–2532. doi:10.1080/09500340701639581.

[12] NIST atomic spectra database, web.
URL http://www.nist.gov/pml/data/asd.cfm

[13] R. Loudon, Quantum Theory of Light, 2nd Edition, Oxford University Press, 1983.

[14] T. N. Anderson, J. K. Magnuson, R. P. Lucht, Diode-laser-based sensor for ultraviolet absorption measurements of atomic mercury, Appl Phys B 87 (2) (2007-04-01) 341–353. doi:10.1007/s00340-007-2604-z.
URL http://dx.doi.org/10.1007/s00340-007-2604-z

[15] M. V. Romalis, E. N. Fortson, Zeeman frequency shifts in an optical dipole trap used to search for an electric-dipole moment, Phys. Rev. A 59 (6) (1999) 4558. doi:10.1103/PhysRevA.59.4547.
URL http://link.aps.org/doi/10.1103/PhysRevA.59.4547

[16] TOPICA Photonics AG, Specifications of Frequncy Quadrupled Diode Lasers, TA-FHG pro (Mar 2009).
URL http://www.toptica.com/

[17] J. Paul, Y. Kaneda, T.-L. Wang, C. Lytle, J. V. Moloney, R. J. Jones, Doppler-free spectroscopy of mercury at 253.7 nm using a high-power, frequency-quadrupled, optically pumped external-cavity semiconductor laser, Opt. Lett. 36 (1) (2011) 61–63. doi:10.1364/OL.36.000061.
URL http://ol.osa.org/abstract.cfm?URI=ol-36-1-61

[18] Y. Chibane, S. K. Lamoreaux, J. M. Pendlebury, K. F. Smith, Minimum variance of frequency estimations for a sinusoidal signal with low noise, Measurement Science and Technology 6 (12) (1995) 1671. doi:10.1088/0957-0233/6/12/004.
URL http://stacks.iop.org/0957-0233/6/i=12/a=004

[19] R. P. Lucht, S. Roy, T. A. Reichardt, Calculation of radiative transition rates for polarized laser radiation, Progress in Energy and Combustion Science 29 (2) (2003) 115–137. doi:10.1016/S0360-1285(02)00044-8.

[20] M. Takeuchi, T. Takano, S. Ichihara, Y. Tkasu, M. Kumakura, T. Yabuzaki, Y. Takahashi, Paramagnetic faraday rotation with spin-polarized ytterbium atoms, Appl. Phys. B 83 (2006) 107–114. doi:10.1007/s00340-006-2136-y.